Precise setting of micro-cavity resonance wavelength by dry etching

Precise setting of micro-cavity resonance wavelength by dry etching

Mehdi Jahed,[a] Johan S. Gustavsson, and Anders Larsson
Photonics Laboratory, Department of Microtechnology and Nanoscience, Chalmers University of Technology, SE-41296 Göteborg, Sweden

(Received 8 February 2019; accepted 3 May 2019; published 22 May 2019)

With an intracavity phase tuning technique, the authors demonstrate <2 nm precision in wavelength setting of vertical-cavity surface-emitting laser (VCSEL) microresonators in the wavelength range 1040–1070 nm using an Ar ion-beam etching process with subnanometer precision in etch depth. This postgrowth fabrication technique for controlling the wavelength of individual VCSELs is promising for the development of monolithic multiwavelength VCSEL arrays with precisely defined wavelengths for wavelength division multiplexed (WDM) optical interconnects and the assembly of compact and high-capacity WDM transmitters. *Published by the AVS.*
https://doi.org/10.1116/1.5092192

I. INTRODUCTION

The vertical-cavity surface-emitting laser (VCSEL) is a micro-cavity laser widely used as a light source in the optical interconnects that provide the connectivity needed in data centers and supercomputers.[1] The need for higher interconnect capacity has led to the development of higher speed VCSELs (Ref. 2) and the use of higher order modulation formats[3] to enable line rates in excess of 100 Gbit/s.[4] For high aggregate capacity, multiple (parallel) fibers are used.

Further improvements of aggregate capacity may come from the use of multiple cores per fiber (spatial division multiplexing) or multiple wavelengths per fiber (wavelength division multiplexing, WDM). A multicore fiber interconnect with a single fiber capacity of 240 Gbit/s has been demonstrated using a six-core fiber and a six-element VCSEL array.[5] Coarse WDM with four channels and 30 nm channel spacing (850, 880, 910, and 940 nm), known as SWDM4, is being implemented[6] and has demonstrated up to 400 Gbit/s (4×100 Gbit/s) single fiber capacity.[7] With WDM being the most promising and scalable approach for higher aggregate capacity and higher bandwidth density, increasing the number of wavelengths per fiber from 4 to 8 and beyond is considered to increase the capacity on a single fiber to ~1 Tbit/s and the aggregate capacity on multiple fibers to ~10 Tbit/s.[8]

Coarse WDM with 30 nm channel spacing requires the assembly and multiplexing of discrete VCSELs fabricated from separate wafers. With an increasing number of channels, this leads to a large footprint. To enable more WDM channels and a small footprint, monolithic multiwavelength VCSEL arrays with reduced channel spacing should be considered. The channel spacing should still be large enough to accommodate the drift in wavelength with temperature (~4 nm from 25 to 70 °C for GaAs-based VCSELs at ~1 μm). With, e.g., 8 nm channel separation and considering the gain-bandwidth of GaAs-based VCSELs, up to six channels (or possibly eight with a smaller channel spacing) should be possible on a single array with good uniformity in terms of threshold current and slope efficiency.

The resonance wavelength of a VCSEL is set by the phase of the reflections from the distributed Bragg reflectors (DBRs) and the propagation phase delay in the cavity separating the DBRs. The latter is controlled by the optical length of the cavity. Any of these phase values can be used to control the emission wavelength. While nonuniform[9] and nonplanar[10] epitaxial growth can be used to induce a variation in wavelength over the wafer, VCSEL designs and fabrication techniques that allow for postgrowth wavelength setting are preferred for precisely controlling the emission wavelength of VCSELs at specific locations on the wafer. Among these techniques, we find nonplanar bonding to control the cavity length of wafer bonded VCSEL,[11] selective oxidation for modifying the cavity length,[12,13] replacement of the top-DBR by a high-contrast grating to control the reflection phase by the grating parameters,[14] the use of an intra-DBR phase tuning layer for controlling the DBR reflection phase,[15–19] and the use of an intracavity phase tuning layer for controlling the cavity length.[20,21]

Intracavity phase tuning is a technique where the cavity length, and therefore the emission wavelength, of a VCSEL with an epitaxial bottom-DBR, active region, and current injection layer is modified before the deposition of a dielectric top-DBR. The cavity length can be changed by thinning either the semiconductor current injection layer above the active region[21] (Fig. 1) or an additional dielectric layer above the current injection layer[20] before top-DBR deposition. While intracavity phase tuning is most effective in controlling the resonance wavelength, it requires precise etching for accurate wavelength control.

Here, we investigate intracavity phase tuning by thinning of the intracavity current injection layer before deposition of the top-dielectric DBR (Fig. 1). The micro-cavity bottom-DBR, active region, and current injection layer are GaAs-based, and the top-dielectric DBR is composed of SiO_2 and TiO_2 layers. For VCSEL micro-cavities in the wavelength range 1040–1070 nm, we demonstrate <2 nm precision in wavelength setting using an Ar ion-beam etching process with subnanometer precision in etch depth. We also investigate the influence of errors in the dielectric DBR layer thicknesses and epi-wafer nonuniformity on the resonance wavelength.

[a]Electronic mail: jahed@chalmers.se

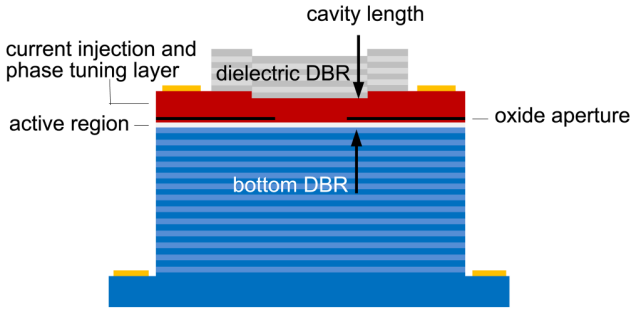

FIG. 1. Intracavity contacted oxide-confined (GaAs-based) VCSEL with dielectric top-DBR. The thickness of the p-type current injection layer (controlled by etching), used as an intracavity phase tuning layer, sets the resonance wavelength.

Finally, we show that the etched surface is as smooth as the unetched. This is essential for high performance VCSELs since a rough surface would cause optical scattering loss, which would degrade performance (increase the threshold current and reduce the slope efficiency) because of the high optical field intensity at the semiconductor–dielectric interface close to the center of the resonator.

The choice of wavelengths (1040–1070 nm) is motivated by opportunities for (1) developing high-speed single-mode VCSELs at these wavelengths[22] and (2) multiplexing in a silicon nitride photonic integrated circuit on silicon with flip-chip integrated multiwavelength VCSEL arrays[23] and multi-channel drivers to form very compact and high-capacity WDM transmitters.

II. ETCHING TECHNIQUE AND PRECISION

As shown in Sec. III, a 1 nm precision in resonance wavelength requires an ~1 nm precision in etch depth for the VCSEL microresonators (GaAs-based with resonance wavelengths at 1040–1070 nm) used in this work.

Etching of semiconductors can be done using wet or dry etching. The proper technique depends on the requirements of etch rate, selectivity, and anisotropy. Since the etch rate of wet etching depends on material composition and doping, and with wet etching being more isotropic, we use in this work dry etching with ions generated in a plasma and accelerated toward the sample by an electric field. The incident

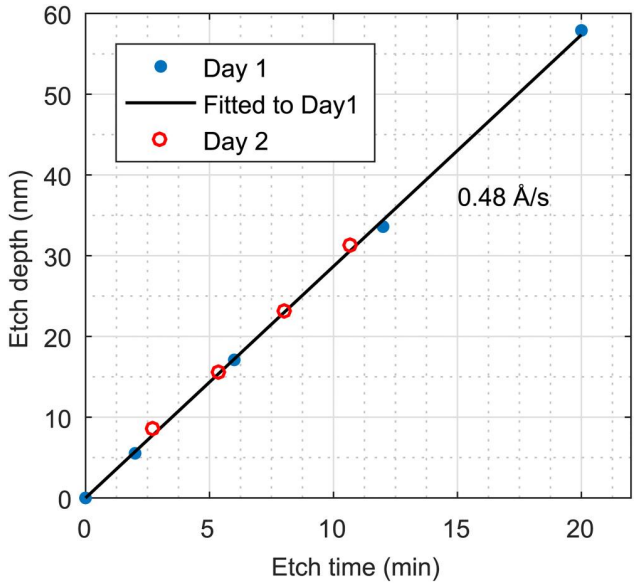

FIG. 2. Measured etch depth vs etch time at two different occasions, spaced in time by a week. The line is a least-square fit to the day 1 measurements.

ions can be neutral or reactive for pure physical (sputtering) or chemical etching, or a combination thereof. Since a precise, stable, and reproducible etch rate, independent of material composition and doping, is needed, we use pure physical etching with neutral ions.

The technique used is Ar ion-beam etching in an Oxford Ionfab 300 Plus system equipped with an electron emitter for neutralizing the ion beam and a rotating sample holder for uniform etching over large areas. The etch rate depends on the applied electric field (ion kinetic energy) and the ion-beam current (ion density). Here, the beam current was set to a low value of 3 mA while the Ar flow rate for both the beam and the neutralizer was set to 4 sccm. The voltage controlling the electric field was set to a low value of 300 V. The sample, which was rotated at 3 rpm during etching, was patterned with photoresist (positive photoresist AZ 1512) to enable measurements of etch depth using atomic force microscopy (AFM). The AFM tool (SPM-Bruker Dimension 1300) was also used for measurements of surface roughness.

The precision and stability of the ion-beam etch process was investigated by measurements of the GaAs etch rate at

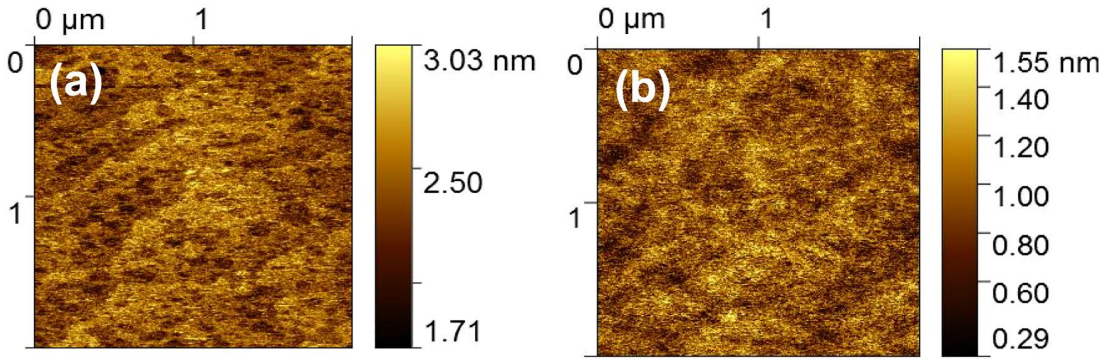

FIG. 3. AFM image of (a) the unetched GaAs surface and (b) the surface after 20 min of Ar ion-beam etching.

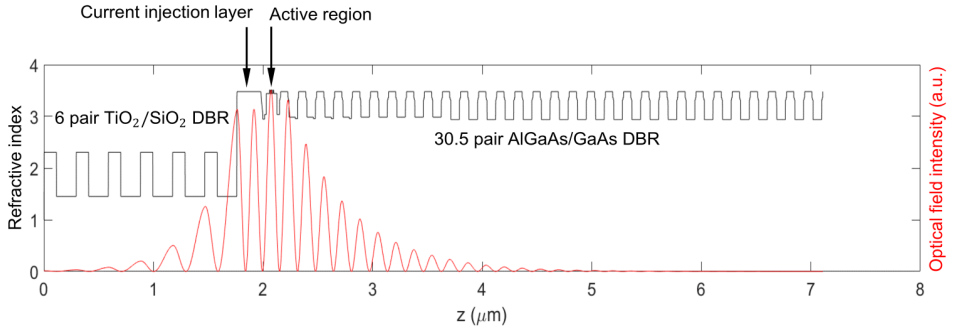

FIG. 4. Variation of refractive index and optical field intensity along the optical axis of the VCSEL with a dielectric top-DBR.

different occasions spaced in time. Figure 2 shows the measured etch depth for different etch times at two different occasions (day 1 and day 2), spaced by a week. On day 1, etching was performed for 2, 6, 12, and 20 min and a straight line was fitted to the measurements, yielding an etch rate of 0.48 Å/s with no noticeable dependence on etch time. On day 2, etching was performed for different etch times from ~2.5 to ~10.5 min, with etch depths deviating less than 1 nm from the depths predicted by the day 1 etch rate. This shows that the ion-beam etch process is stable and reproducible, with subnanometer precision in etch depth over the depths needed (up to 40 nm) to set the microresonator wavelength between 1040 and 1070 nm for our particular VCSEL design (see Sec. III).

The roughness of unetched and etched surfaces was measured by AFM over $2 \times 2\,\mu m^2$ areas. Figure 3 shows AFM images of the unetched surface and a surface after 20 min of Ar ion-beam etching. The unetched surface has an rms roughness of 194 ± 36 pm, while the etched surface has an rms roughness of 204 ± 23 pm. The small roughness (subnanometer) and very small increase of roughness (within the measurement accuracy) after etching show that the slow etch rate (low ion-beam current and low beam voltage) enables not only a precise etch depth but also very smooth surfaces.

III. INTRACAVITY PHASE TUNING AND WAVELENGTH SETTING

The epitaxial half-VCSEL structure used for the intracavity phase tuning experiments consists of a 30.5 pair of AlGaAs/GaAs n-type bottom-DBR and an undoped active region with partially strain-compensated InGaAs/GaAsP quantum wells (QWs) with a p-type GaAs intracavity current injection layer on top. The active region includes three QWs with photoluminescence wavelength at 1045 nm. A six-pair SiO_2/TiO_2 dielectric DBR is deposited on top of the current injection layer to form the VCSEL resonator. The thickness of the cavity (active region + current injection layer) is chosen to set the resonance wavelength at 1070 nm before thinning of the current injection layer. The epitaxial structure was fabricated using metal-organic chemical vapor deposition and the dielectric DBR was deposited by sputtering.

The full VCSEL structure with the optical field intensity along the optical axis of the resonator is shown in Fig. 4. The high field intensity at the semiconductor–dielectric interface illustrates the importance of having a smooth surface of the current injection layer.

The resonance wavelength is blue-shifted when the thickness of the current injection layer is reduced (by Ar ion-beam etching, before top-dielectric DBR deposition). The calculated shift in wavelength as a function of etch depth is shown in Fig. 5. For these calculations, an effective index model[24] was used with the refractive index of the epitaxial layers calculated using the Afromowitz model[25] and the refractive index of the sputtered dielectric DBR layers measured using ellipsometry (1.488 for SiO_2 and 2.259 for TiO_2 at 1055 nm). The effective index model provides an accurate value for the resonance wavelength of an oxide-confined VCSEL as long as the oxide aperture is not too small. The near linear 0.95 nm shift in wavelength per nanometer of etching deduced from Fig. 5 illustrates the close to ±1 nm precision in etch depth needed to control the resonance wavelength to within ±1 nm.

For measurements of the resonance wavelength of fabricated microresonators with different thicknesses of the current injection layer, we used reflectance spectroscopy. A broad-

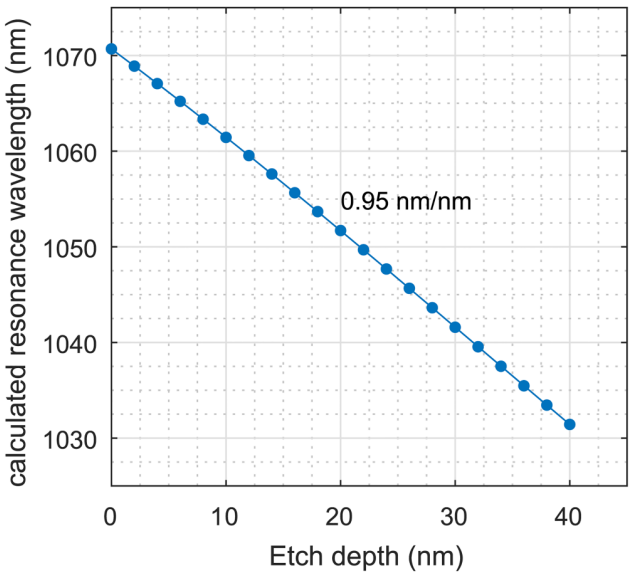

FIG. 5. Calculated resonance wavelength vs etch depth of the current injection layer.

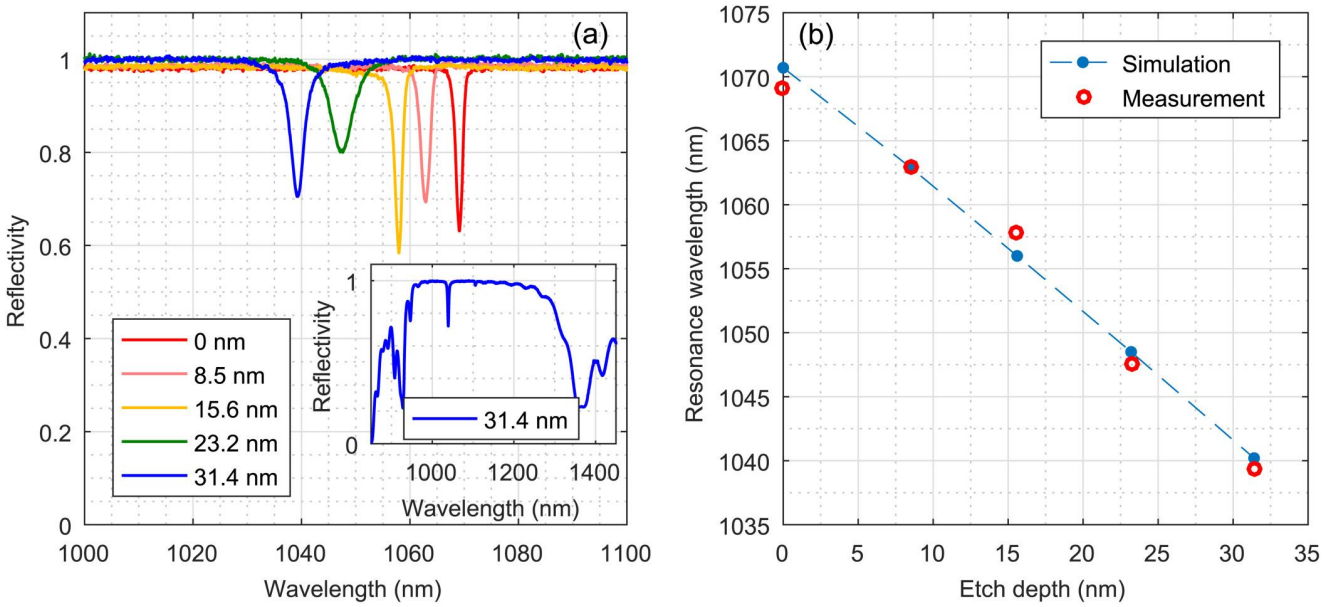

FIG. 6. (a) Reflectance spectra recorded for the five different samples, showing the reflectance dips that define the resonance wavelengths. The inset to the left lists the etch depths, while the inset to the right shows the reflectance spectrum for the sample with 31.4 nm etch depth over a wider spectral range. (b) Measured etch depths and resonance wavelengths for all the samples (red circles). The calculated dependence of wavelength on etch depth (from Fig. 5) is shown by the blue dots and the dashed blue line.

spectrum light source was coupled to the outer cores of a multicore optical fiber with the other end of the fiber held at a distance to the surface of the microresonator. Reflected light was collected by the center core and sent to an optical spectrum analyzer for spectral analysis. The recorded reflectance spectrum was calibrated against that recorded from measurements on a gold surface. The dip in the reflectance spectrum within the stop-band of the DBRs defines the resonance wavelength.

Five samples from the half-VCSEL wafer were etched at different times using the Ar ion-beam etching technique presented in Sec. II. The etch times were 0, 160, 320, 480, and 640 s, which should produce equidistant resonance wavelengths with a spacing of 7.3 nm (from Figs. 2 and 5). Each sample had a photoresist pattern to enable measurements of the etch depth by AFM after etching and removal of the photoresist. The measured etch depths for the etched samples were 8.5, 15.6, 23.2, and 31.3 nm, which again is within ±1 nm of the expected values from the measured etch rate. Finally, the dielectric DBR was deposited on all samples simultaneously and the resonance wavelength of each sample was determined using the reflectance spectroscopy [Fig. 6(a)]. The measured resonance wavelengths and etch depths are shown in Fig. 6(b). The maximum deviation between measured and calculated wavelengths is 1.9 nm. This demonstrates that the resonance wavelength can be controlled to within less than ±2 nm using these fabrication techniques for intracavity phase tuning.

The measured precision in wavelength setting (±2 nm) is less than that predicted from the precision in etching only (±1 nm). The reason is that there are other sources of error. One is the inherent nonuniformity in the thickness of the epitaxial layers over the wafer. A spectral reflectance map for the central part of the as-grown wafer, from which the samples were cut, revealed a variation in thickness of the cavity layers corresponding to a variation in resonance wavelength for the full VCSEL structure of ∼±0.5 nm.

Another and more significant source of error is the accuracy in thickness and refractive index for the SiO_2 and TiO_2 layers used in the dielectric DBR. Deviations in thickness from a quarter-wavelength (ideally 182 and 116 nm, respectively, at a center wavelength of 1055 nm) lead to a change in the reflection phase and therefore in the resonance wavelength. Errors in the first dielectric DBR pair have the largest impact, while errors in pairs further away from the cavity have less impact. This is shown in Table I, where the shifts in resonance wavelength caused by a 5 nm error in layer thicknesses (2.8% error in SiO_2 layer thickness and 4.3% error in TiO_2 layer thickness) in the first three pairs are listed. Such an error in the first pair shifts the wavelength by 1.4 nm, while the shift caused by this error in the other pairs is less.

To minimize the errors in the thickness of the dielectric layers in the experiments in Fig. 6, the thickness and refractive index of each layer were measured by ellipsometry

TABLE I. Shifts of the resonance wavelength ($\Delta\lambda_r$) caused by 5 nm error in thickness (Δd) of the dielectric layers in the first three pairs of the dielectric DBR.

Pair #	Δd_{SiO_2} (nm)	Δd_{TiO_2} (nm)	$\Delta\lambda_r$ (nm)
1	5	5	1.4
2	5	5	0.6
3	5	5	0.3